University of Groningen

Quantum Sensing for Detection of Zinc-Triggered Free Radicals in Endothelial Cells

Wojtas, Daniel; Li, Runrun; Jarzębska, Anna; Sułkowski, Bartosz; Zehetbauer, Michael; Schafler, Erhard; Wierzbanowski, Krzysztof; Mzyk, Aldona; Schirhagl, Romana

IMPORTANT NOTE: You are advised to consult the publisher's version (publisher's PDF) if you wish to cite from it. Please check the document version below.

Document Version
Publisher's PDF, also known as Version of record

Publication date:
2023

[Link to publication in University of Groningen/UMCG research database](#)

Quantum Sensing for Detection of Zinc-Triggered Free Radicals in Endothelial Cells

Daniel Wojtas, Runrun Li, Anna Jarzębska, Bartosz Sułkowski, Michael Zehetbauer, Erhard Schafler, Krzysztof Wierzbanowski, Aldona Mzyk,* and Romana Schirhagl*

Oxidative stress originating from the overproduction of free radicals poses a major threat to cell fate, therefore it is of great importance to address the formation of free radicals in cells subjected to various pathological stimuli. Here we investigate the free radical response of endothelial cells to biodegradable zinc. In addition to the standard free radical assays, relaxometry was used for determining the production of free radicals in cells exposed to non-physiological concentrations of zinc ions. The cellular morphology, intracellular zinc accumulation, as well as the levels of reactive oxygen/nitrogen species, are determined using standard fluorescent methods. For endothelial cells subjected to 50% zinc extracts, deviations from the normal cell shape and cell agglomeration tendency are observed. The culture medium containing the highest amount of zinc ions caused nuclei fragmentation, blebbing, and cell shrinkage, indicating cell death. A potential explanation for the observed phenomena is an overproduction of free radicals. In the case of 1% and 10% zinc extracts, the formation of free radicals is clearly confirmed by relaxometry, while the results obtained by using fluorescent techniques are unambiguous. It is revealed that high concentrations of zinc ions released from biodegradable samples induce a deleterious effect on endothelial cells.

1. Introduction

Over recent years, various zinc-containing materials have attracted considerable attention in the biomedical field as they show diverse and wide-ranging potential applicability. Biodegradable implants and fixation devices could benefit from the use of zinc-based biomaterials, while zinc oxide nanoparticles (NPs) might be of vast importance for anticancer treatments, drug delivery, or bioimaging.[1,2] Generally, zinc and its alloys are corrosion resistant, enabling a steady, controlled disintegration of implanted materials. On the other hand, zinc oxide NPs have been widely investigated owing to their therapeutic effects. In addition, a great deal of research has been devoted to zinc-enriched surfaces since they tend to lower the adhesion of microorganisms, opening a new path in the prevention of bacteria-associated infections and diseases.[1–3] From the point of view of biological significance, zinc is known to play

D. Wojtas
Faculty of Medicine
Masaryk University
Kamenice 753/5, Brno 625 00, Czechia

D. Wojtas, K. Wierzbanowski
Faculty of Physics and Applied Computer Science
AGH University of Science and Technology
al. Mickiewicza 30, Kraków 30-059, Poland

R. Li, A. Mzyk, R. Schirhagl
Department of Biomedical Engineering, University of Groningen
University Medical Center Groningen
Antonius Deusinglaan 1, Groningen 9713AW, The Netherlands
E-mail: aldonamzyk@googlemail.com; romana.schirhagl@gmail.com

A. Jarzębska
Institute of Metallurgy and Materials Science
Polish Academy of Sciences
ul. Reymonta 25, Kraków 30-059, Poland

B. Sułkowski
Faculty of Non-ferrous Metals
AGH University of Science and Technology
al. Mickiewicza 30, Kraków 30-059, Poland

M. Zehetbauer, E. Schafler
Faculty of Physics
University of Vienna
Boltzmanngasse 5, Wien 1090, Austria

A. Mzyk
Department of Health Technology
Danish Technical University
Ørsteds Plads, Kongens Lyngby DK-2800, Denmark

ADVANCED
SCIENCE NEWS

www.advancedsciencenews.com

ADVANCED
QUANTUM
TECHNOLOGIES

www.advquantumtech.com

an important role in the functioning of the immune system, DNA transcription, cell division, breakdown of carbohydrates, and iron transport. Moreover, its deficiency is believed to be linked to retardation in growth and development as well as alterations in cognitive functions.[4,5] Zinc and its alloys are generally considered to be biocompatible, however, with the advent of various zinc-based bulk materials, coatings, and NPs for biomedical purposes, the impact of zinc ions on cells at the nanoscale should be carefully revisited.

Generally, zinc ions are well-known as antioxidants, protecting endothelial cells from inflammatory cytokines and polyunsaturated lipids, as well as stabilizing membranes and inhibiting the enzyme NADPH oxidase.[6,7] On the contrary, excessive Zn^{2+} in cells has been related to ROS generation,[8,9] although the exact mechanism explaining this phenomenon has yet to be fully understood. ROS encompasses a great deal of highly-reactive, oxygen-containing molecules formed during an incomplete reduction of oxygen in a cell.[10] They can be either free radicals, e.g., $O_2^{\bullet-}$ or $HO^{\bullet}$, or non-radical molecules having the ability to generate free radicals, e.g., H_2O_2 or $^1O_2$. The reason behind the extraordinary reactivity of radical species is an unpaired electron present in the outer shell of their atoms.[11] The biological significance of free radicals is profound as they influence signal transduction or take part in tissue defense mechanisms, realized by immune cells, such as neutrophils or macrophages. Nonetheless, the overproduction of ROS results in oxidative stress which, finally, may cause irreversible cell damage or even their death. Hence, a balance between free radical generation and elimination is of immense significance.[12]

Since free radicals are short-lived, unstable, and produced in small concentrations, their detection becomes arduous. Fluorescence techniques represent one of the most common approaches used to detect free radicals. However, the inherent sensitivity of dyes to photo-oxidation, bleaching, and changes in the chemical environment pose a challenge in determining free radical levels in cells.[12] Apart from fluorescent probes, free radicals can be also detected by electron spin resonance (ESR) spectroscopy. Nonetheless, high spatial resolution measurements are limited while using ESR. Diamond magnetometry (DM) is a technique that is based on the nitrogen-vacancy (NV) center, a defect in diamond, which changes its optical properties based on its magnetic surrounding. Since optical signals can be detected more sensitively, the method stands out in terms of its sensitivity. The method is so sensitive that even the small signal of single nuclear spins can be detected.[13,14] In physics, DM has been employed to the measurements of magnetic nanostructures, domain walls, or magnetic vortices.[15] In biomedical sciences, DM has been successfully applied to detect proteins, the magnetic signal of a cell slice, and magnetotactic bacteria.[16–18] Relaxometry is a specific mode of diamond magnetometry that is sensitive to paramagnetic species. The principle of relaxometry has first been demonstrated for detecting paramagnetic Gd^{3+} ions in solution.[19] Since then, the technique has been used for example to measure magnetic structures, superconductors, different paramagnetic ions, or ferritin molecules.[19–25] In combination with responsive coatings, which vary in spin label concentration, relaxometry may be used to detect redox processes and pH changes.[26–28] In cells, relaxometry allows detection of free radicals. This has been demonstrated for instance in mea-

surements in yeast cells, sperm cells, immune cells, endothelial cells, and bacteria, and during the response of cells to viruses or drugs.[29–35] Analogously to T_1 measurements in conventional Magnetic Resonance Imaging (MRI), the magnetic noise coming from the NV center surroundings is detected in relaxometry.

Herein, this method has been used for the very first time to detect the real-time generation of free radicals in endothelial cells subjected to various amounts of zinc ions released from biodegradable samples. The technique has been utilized in combination with two standard fluorescent probes employed typically to analyze the formation of intracellular reactive species. Eventually, relaxometry measurements allowed us to reveal the nanoscale impact of metal ions on cells, i.e., the formation of free radicals. Compared to the fluorogenic probes our method does not suffer from photobleaching, and is not sensitive to reactive but non-radical species. Our method is also less affected by other fluorescent molecules. Finally, our method reveals the current radical load rather than the history of the sample.

2. Experimental Section

2.1. Material Development

A billet of pure zinc (99.999%) with a diameter of 38 mm in the as-cast state was extruded at 200 °C to a rod with 10 mm in diameter with a true strain of 2.67. Prior to the biological investigations described here, the material was cut, abraded, and polished, following standard metallographic procedures. In doing so, a set of SiC papers up to 4000 grit as well as alcohol-based diamond suspensions were used. Owing to the degradability of zinc, before cell culturing, zinc-bearing extracts were prepared and stored in a manner similar to those described in[36,37] by placing cell culture medium (CCM, Endothelial Basal Medium, CC3156, Lonza) on a single sample surface with a medium-to-area ratio of 1.25 mL cm^{-2}. The immersed discs were kept for 24 h at 37 °C in a humidified atmosphere of 5% CO_2. During this process, zinc ions are released into the medium and this solution is termed the 100% zinc extract. Four different zinc extracts, i.e., 100%, 50%, 10%, and 1%, upon serial dilution with the CCM were produced. After preparation, the extracts were stored at 4 °C, but no longer than 3 days after incubation. The actual concentrations of zinc ions within the examined extracts, as shown in **Table 1**, were detected by using the inductively coupled plasma mass spectrometry (ICP-MS, Thermo Fisher Scientific) technique. For the ICP-MS studies, a standard addition-method with six calibration points and the use of a 100 μL sample per point was applied. The

Table 1. The contents of extracts.

Extract concentration [% v/v]	CCM volume [% v/v]	Zn^{2+} concentration $[\frac{\mu g}{mL}]$
100%	0%	23.48
50%	50%	11.74
10%	90%	2.35
1%	99%	0.24

ADVANCED
SCIENCE NEWS

www.advancedsciencenews.com

ADVANCED
QUANTUM
TECHNOLOGIES

www.advquantumtech.com

samples were diluted with an aqueous solution of 0.1% HNO_3 containing internal standards (Scandium and Germanium).

2.2. Fluorescent Nanodiamonds

Diamonds for T_1 measurements were fluorescent nanodiamond particles (FNDs) with a mean hydrodynamic diameter of 70 nm and a flake-like structure (Adamas Nanotechnologies, NC, USA). According to the producer, FNDs are obtained through high pressure – high temperature (HPHT) synthesis and grinding. Then, particles are irradiated with 3MeV electrons at a fluence of 5×10^{19} e cm^{-2} and annealed at a temperature exceeding 700 °C.[38] As a result, they contain $\approx$500 NV^- centers per particle. The surface of FNDs is oxygen-terminated because in the last stage of their processing they are treated with oxidizing acids. FNDs are known to be fully biocompatible and exhibit excellent charge stability and infinitely stable fluorescence.[39–41] Hence, they have been successfully applied for labeling and imaging.

2.3. Cell Culture

Within the present study, human umbilical vein endothelial cells (HUVECs, CC2519, Lonza), obtained by the courtesy of the Endothelial Facility, University of Groningen, were used for all investigations. HUVECs were cultured in the EGM-2MV solution (CC3202, Lonza), consisting of EBM-2 Basal Medium (CC3156, Lonza) as well as EGM-2 MV supplements and growth factors (CC4147, Lonza) at 37 °C with 5% CO_2 until 90% confluence.

2.4. Cell-Material Interactions

Cell-material interactions were determined upon 4 and 24 h of incubation with zinc extracts. Before imaging, the cells were fixed with 4% paraformaldehyde solution for 10 min and permeabilized with 0.1% Triton X-100 (Sigma) for 7 min. Following washing with fresh phosphate buffered saline (PBS), HUVECs were stained with FITC-phalloidin (Sigma) for 30 min and DAPI (Sigma) for 5 minutes so cell F-actin fibers of cytoskeleton and cell nuclei, respectively, could be observable. Finally, the cells were rinsed with PBS to remove dye residues and imaged. Cell morphology and proliferation were analyzed based on images acquired with a confocal laser scanning microscope (CLSM) Stellaris 8 Leica Microsystems. The excitation/emission wavelengths for FITC-phalloidin and DAPI were 495/513 nm and 340/488 nm, respectively. The captured images were processed by employing the LAS X software. In addition, the Image Region Analyzer toolbox in MATLAB was employed for quantitative analysis of the CLSM-derived data. The nuclear fragmentation index and cell shrinkage ratio were calculated upon image binarization as the mean number of pixels constituting nucleus and cytoskeleton, respectively, with respect to the reference. In doing so, 20 binarized objects were taken into consideration. The number of cell blebs and the percentage of blebbing were computed for a series of six images taken from various places of an imaged well. The former was additionally referenced to the image area.

2.5. Zinc Accumulation

Upon either 4- or 24-h incubation with zinc extracts, the cells were exposed to the FluoZin-3 indicator (Thermo Fisher Scientific), a Zn^{2+}-selective probe in a cell-permeant form, in order to reveal the extent of intracellular accumulation of zinc. The indicator, consisting of acetoxymethyl (AM) ester, was prepared according to the manufacturer's protocol. HUVECs were incubated with the AM ester at the concentration of 2.5 μM for 30 min at 20 °C. Subsequently, they were rinsed with CCM and incubated for further 30 min in CCM until de-esterification of intracellular AM esters was completed. Finally, a CLSM Stellaris 8 Leica Microsystems was employed for image acquisition. The FluoZin-3 excitation and emission wavelengths used were 494 and 516 nm, respectively. The mean fluorescence intensity, reflecting intracellular zinc accumulation, was quantified using the ImageJ software. A single mean intensity was computed using the formula for corrected total cell fluorescence,[42] which is calculated as the integrated density minus the product of the selected area and the mean fluorescence of background readings. For each image, five distinct background areas were employed for normalization against autofluorescence. Finally, the mean intensities were related to the control group.

2.6. DHE Assay

A DHE (Dihydroethidium) Assay Kit (abcam), containing a fluorescent probe, was utilized in order to inspect the generation of ROS, mainly superoxide, $O_2^{\bullet-}$, in endothelial cells exposed to zinc ions. In general, a DHE indicator gets oxidized by either superoxide to form 2-hydroxyethidium (2-OH$^-$E$^+$) or by non-specific oxidation with other sources of ROS to form ethidium (E$^+$). Both reaction products bind to DNA to give off bright red fluorescence. Following 4- or 24-h incubation with zinc extracts at 37 °C and 5% CO_2 the cells were treated with a DHE-containing CCM solution at the concentration of 10 μM (from a DHE stock solution). Consequently, the cells were incubated for 10 min at 37 °C and 5% CO_2 and rinsed with ice-cold CCM before image acquisition. The fluorescence images were taken from at least ten randomly selected cells per well using a CLSM Stellaris 8 Leica Microsystems. The excitation/emission wavelengths were set to 514/580 nm, as described. [32] Finally, the mean fluorescence intensity, regarded as a function of the ROS level generated by a cell, was determined by using the ImageJ open-source software. A specific intensity was calculated based on the corrected total cell fluorescence approach, as described above.

2.7. DAF-FM Assay

DAF-FM Diacetate (4-Amino-5-Methylamino-2″,7″-Difluorofluorescein Diacetate, Thermo Fisher Scientific), a fluorescent indicator developed to detect the intracellular nitric monoxide, $NO^{\bullet}$ and its derivatives, was used in order to determine the impact of zinc ions on reactive nitrogen species (RNS) generation in cells. Upon 4- or 24-h incubation of HUVECs with zinc extracts at 37 °C and 5% CO_2, the cells were treated with DAF-FM at a concentration of 0.5 μM (from a DAF-FM stock solution). Subsequently,

**ADVANCED
SCIENCE NEWS**

www.advancedsciencenews.com

**ADVANCED
QUANTUM
TECHNOLOGIES**

www.advquantumtech.com

they were rinsed with fresh CCM and incubated anew for 15 min to finalize the intracellular DAF-FM diacetate de-esterification. During the process, the non-permeable, nonfluorescent DAF-FM is formed and converted to the highly fluorescent benzo-triazole form in the presence of NO$^\bullet$. Finally, the fluorescence images were captured from a set of 10 randomly selected cells per well using a CLSM Stellaris 8 Leica Microsystem. The excitation/emission wavelengths of 495/515 nm were chosen for imaging, thus in a manner similar to that described.[32] The relative levels of intracellular RNS were quantified from the mean fluorescence intensity of DAF-FM by employing the ImageJ open-source software. The specific intensities were quantified as corrected total cell fluorescence, in a manner described above.

2.8. Relaxometry

Prior to T$_1$ measurements, FNDs at the concentration of 2 μg mL^{-1} were internalized by cells during 4-h incubation at 37 °C and 5% CO$_2$. At the end of incubation, the cells were washed with fresh culture medium and exposed to zinc-containing extracts for either 4 or 24 h. A single confocal scan was performed with a 532 nm laser (50 μW at the position of the sample under continuous illumination) in order to detect FNDs inside a particular endothelial cell.[29] A ×100 magnification oil objective (Olympus, UPLSAPO 100XO, NA 1.40) and an acousto-optical modulator (Gooch & Housego, model 3350-199) were used to conduct the pulsing sequence. All of the T$_1$ measurements were carried out under static conditions at room temperature. To perform a T$_1$ measurement, NV centers are brought into the bright m$_s$ = 0 state of the ground state and then it is checked after different dark times how long the NV centers remain in this state by probing the fluorescent intensity after different dark times. More specifically, the NV^- centers were pumped to the bright ground state with a 5 μs long laser pulse. Afterwards, probing (the first 0.6 μs were used as read window) if the NV$^-$ centers were still there or had returned to the darker equilibrium between the m$_s$ = ±1 and the m$_s$ = 0 state was made. The spin relaxation dynamics follow a decreasing exponential whose time constant is called the spin relaxation time, or T$_1$.[43] This process gets shortened in the presence of free radicals in the surrounding area. Thus, the relaxation time (= T$_1$) reveals the free radical concentration. Each T$_1$ measurement takes on the order of milliseconds. However, to obtain a good signal-to-noise ratio, each measurement was repeated 10 000 times, with the dark times varying from 200 ns to 10 ms. Since the particles are moving through the cell, every 3 s the setup performed automated re-centering to make sure that the particle is not lost. A single measurement took ≈10 min. The experiments were carried out by using a custom made magnetometry setup, whose principles and usage can be found elsewhere.[22,29,34] The collected data was processed using our original MATLAB script. The relaxation curves were fitted by the double exponential fit function for extracting T$_1$ as done in our previous study.[22] In addition to T$_1$ measurements in cells, T$_1$ values in extracts alone were also recorded in order to check whether zinc-containing media may influence the results of T$_1$ measurements. In doing so, the value of T$_1$ was first measured by using FNDs covering a well and then FNDs immersed in the particular extract.

2.9. Statistical Analysis

The obtained data was checked with regard to its statistical significance by using the GraphPad prism v. 8 software. In doing so, the differences between the analyzed probes were compared with a one-way ANOVA. A P-value of < 0.05 was chosen as the threshold for statistical significance.
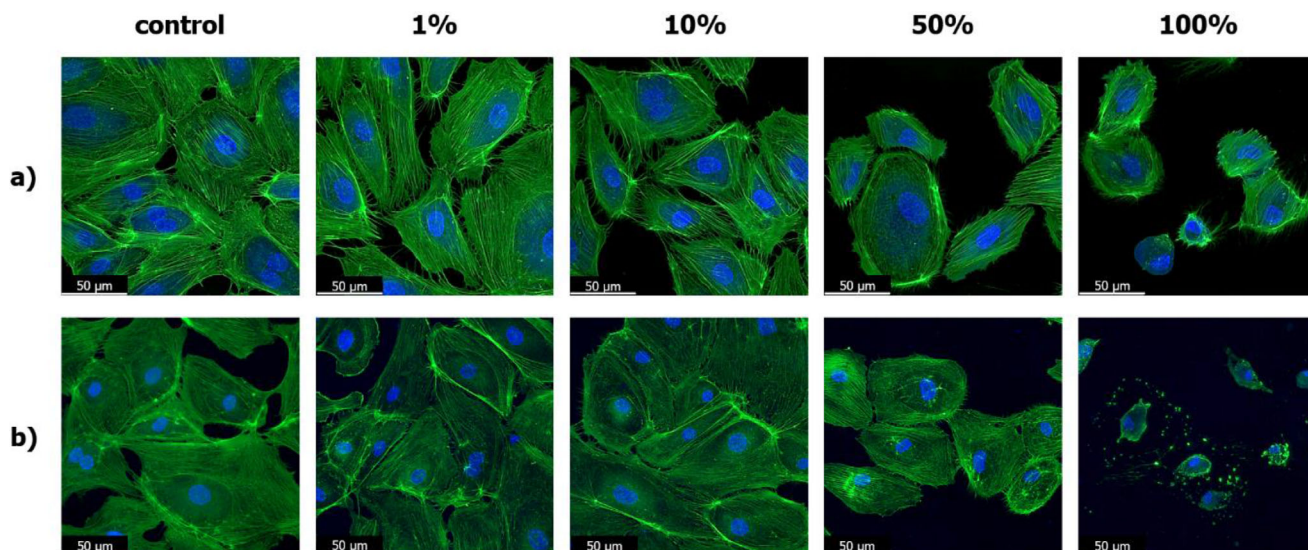
3. Results

3.1. Cell-Material Interactions

Representative confocal images displaying cell behavior under exposure to different zinc concentrations are illustrated in **Figure 1**. In the control group, cells were forming nearly monolayers, regardless of the incubation time. HUVECs treated with extracts containing either 1% or 10% of zinc ions exhibited normal, oblong morphology with easily observable actin stress fibers and well-defined pseudopodia. However, the cells subjected to 10% extract were no longer evenly distributed on the imaged surface as clusters, as well as single cells were seen. The CLSM images collected for HUVECs exposed to the 50% and 100% extracts clearly showed the impact of higher zinc amount on endothelial cells. Upon culturing in the 50% extracts, cells were able to grow and proliferate, yet they were no longer grouped in sizable clusters. Some of them manifested abnormal, close-to-rounded, or globular shapes which undoubtedly implies pathological influence of excessive zinc ions. The absence of filopodia should be also highlighted. In the case of cells cultured in 100% extract for 4 h, barely a couple of HUVECs were viewed and almost neither of them exhibited proper size and shape. Upon 24-h incubation, endothelial cells did not survive in the extracts bearing the highest amount of zinc ions as the signs of cell death, including shrinkage, bleb formation, and nuclear fragmentation, were noticeable. As seen, both from the CLSM-derived morphologies and the quantitative data presented in Figure S1 (Supporting Information), the deleterious impact of 100% zinc extracts on HUVECs is evident.

3.2. Zinc Accumulation

The morphologies of HUVECs cultured in zinc extracts and stained with a zinc-specific fluorescent probe are shown in **Figure 2**, while their normalized fluorescence intensities are displayed in **Figure 3**. The fact that the control group gave off a fluorescent signal proves that zinc, in the form of various compounds, is naturally present within some of the endothelial cell compartments. Upon 4-hour incubation, we observed a progressive rise in the normalized fluorescence intensity with an increase in the concentration of zinc extract. However, the differences in the intracellular zinc levels between cells exposed to 1% and 10% zinc extracts were statistically insignificant suggesting that ions contained in more diluted extracts are either evenly distributed in cellular organelles and/or bound to other biomolecules. Interestingly, after 24 h of incubation, the intensities arising from cells subjected to 1% and 10% zinc extracts were in the range of the control. Considering cellular morphology and the extent of proliferation, this might indicate a positive role of small, yet non-physiological amounts of zinc ions in

2300174 (4 of 13)

**ADVANCED
SCIENCE NEWS**

www.advancedsciencenews.com

**ADVANCED
QUANTUM
TECHNOLOGIES**

www.advquantumtech.com

Figure 1. Morphology of HUVECs incubated for a) 4 h, b) 24 h with zinc-bearing extracts. The cell nuclei were stained with DAPI (blue color) and F-actin of the cytoskeleton was stained with FITC-phalloidin (green color).

culture media. Overall, the mean fluorescence intensities were always greater upon 4-h incubation than after 24-h incubation. This suggests that as treatment with zinc ions gets extended, endothelial cells take up the excessive amounts of intracellular zinc ions. At the same time, a surge in the mean fluorescent intensity observed for the cells treated with 100% extracts, regardless of the incubation time, implies that the occurring cell death may be zinc-initiated. Here it is important to note, that an increased zinc concentration in dead cells might also occur due to increased cell permeability. Thereby, while the higher amount of zinc would not be indicative of zinc being the cause of cell death, together with the fact that clear signs of cell death are seen in these samples renders such an explanation likely. The phenomenon is supported by the fact that majority of the cellular compartments contained zinc
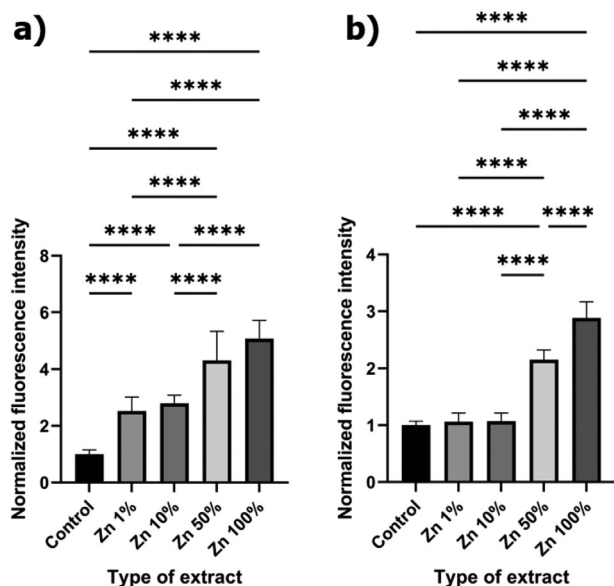
in their structure, as evidenced by the CLSM images. However, it is worth noting that Zn^{2+} might react with various anions, forming, e.g., zinc oxide, zinc salts, and other oxidation states which might ultimately cause toxicity instead of Zn^{2+} itself.[44,45]

3.3. DHE Assay

The CLSM-derived morphologies of HUVECs treated with DHE solution are illustrated in **Figure 4**, while their normalized fluorescence intensities are displayed in **Figure 5**. In addition, the estimated concentrations of ROS based on the approach described[32] are shown in Figure S2 (Supporting Information). All of the examined cell cultures, including the control,
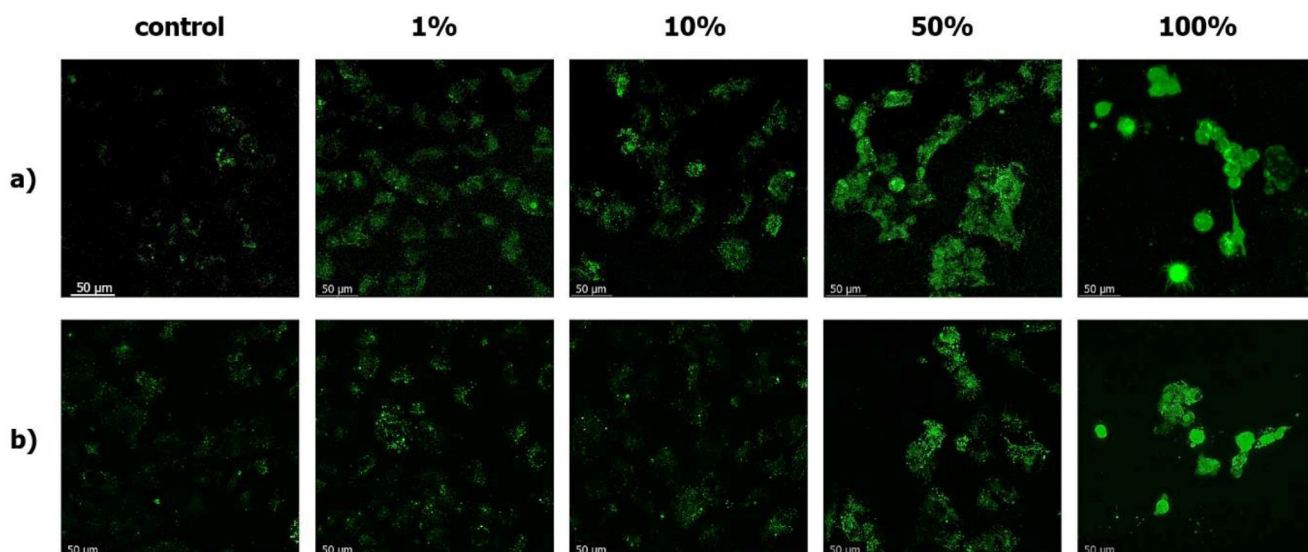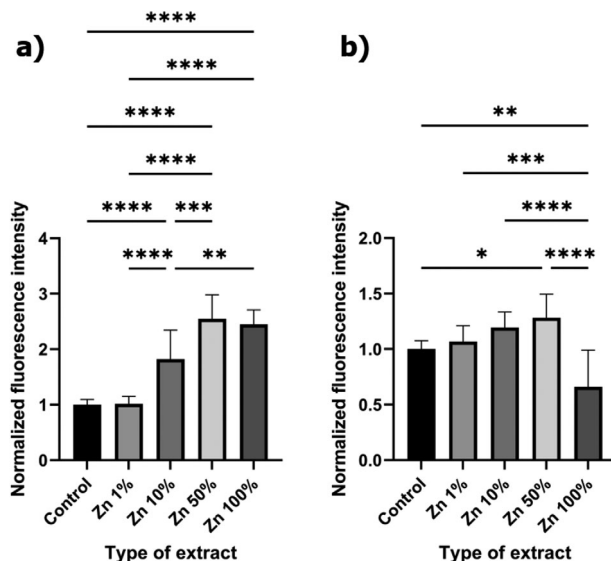

Figure 2. Morphology of HUVECs incubated for a) 4 h, b) 24 h with zinc-bearing extracts and stained with the FluoZin-3 fluorescent probe.

**ADVANCED
SCIENCE NEWS**

www.advancedsciencenews.com

**ADVANCED
QUANTUM
TECHNOLOGIES**

www.advquantumtech.com

Figure 3. Normalized fluorescence intensity evaluated for cells treated with various zinc-containing extracts for a) 4 h, b) 24 h and the FluoZin-3 fluorescent probe. The experiments were performed in six replicates for each variant. Data are presented as means ± standard deviation. The asterisks denote statistical significance (* $p < 0.05$, ** $p < 0.01$, *** $p < 0.001$, **** $p < 0.0001$).
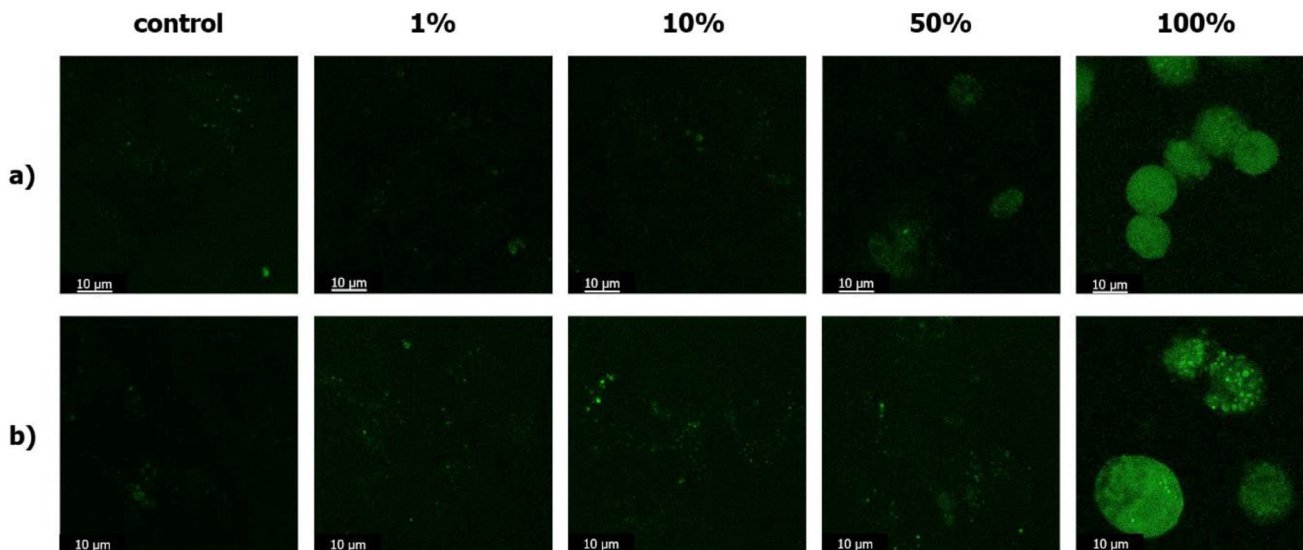
Figure 5. Normalized fluorescence intensity evaluated for cells treated with various zinc-containing extracts for a) 4 h, b) 24 h and the DHE solution. Experiments were performed in six replicates for each variant. Data are presented as means ± standard deviation. The asterisks denote statistical significance (* $p < 0.05$, ** $p < 0.01$, *** $p < 0.001$, **** $p < 0.0001$).

generated detectable amounts of superoxide and its derivatives (henceforth, we use the term ROS with respect to DHE assay since, as discussed further, not only $O_2^{\bullet-}$ but also other ROS might be detected by the kit), although at various concentrations. Upon 4-hour culturing with zinc extracts, the production of ROS in HUVECs was always more pronounced than at 24-h incubation. The fact that no statistical significance in fluorescence intensity was noted between cells exposed to 1%, 10%, and 50% zinc extracts after a prolonged treatment suggests that ROS production occurs mainly during the early stage of incubation. Overall, in-

creasing the amount of zinc ions in CCM caused endothelial cells to produce a gradually higher concentration of ROS except for HUVECs subjected to 100% zinc extracts. Upon 4-hour incubation, the level of ROS generated in cells treated with 50% and 100% zinc extracts was the greatest and the differences between those groups were statistically insignificant. This indicates that, as expected, ROS production is enhanced in cells experiencing clearly visible signs of cell death, including cytoskeleton condensation or blebbing. The excessive amount of intracellular ROS formation could be linked to HUVECs not exhibiting typical morphology and their inability to form agglomerates. However, after
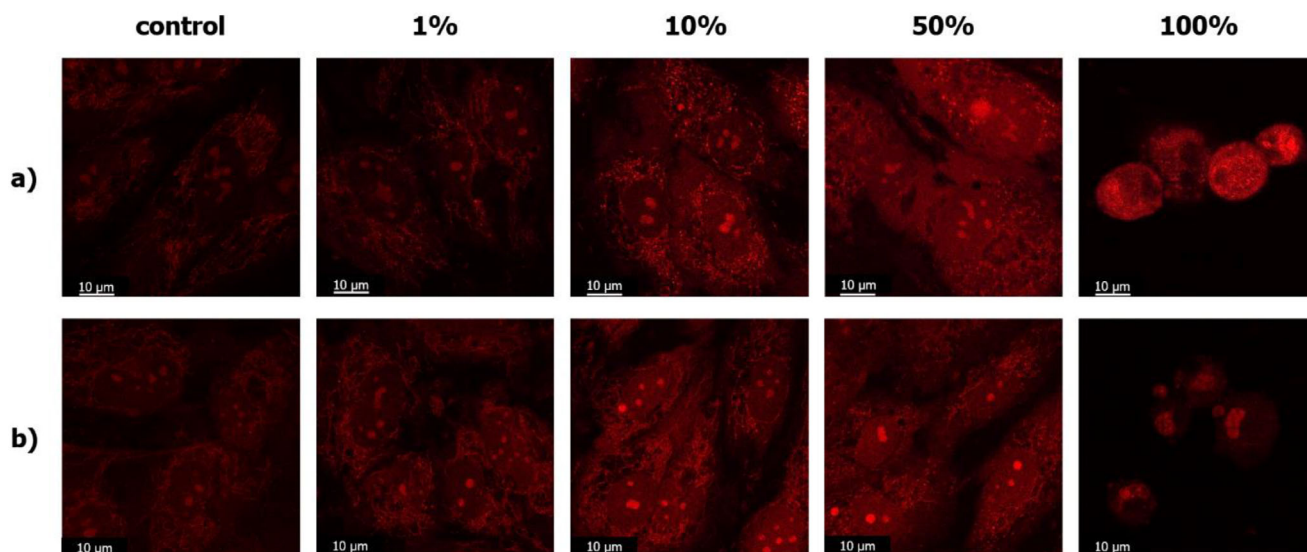
Figure 4. Morphology of HUVECs incubated for a) 4 hours, b) 24 hours with zinc-bearing extracts and treated with DHE solution.

ADVANCED
SCIENCE NEWS

www.advancedsciencenews.com

ADVANCED
QUANTUM
**TECHNOLOGIES**

www.advquantumtech.com

Figure 6. Morphology of HUVECs incubated for a) 4 h, b) 24 h with zinc-bearing extracts and treated with DAF-FM solution.

24 h of incubation, a two-fold decrease in the normalized fluorescence intensity was noted for cells cultured in 100% zinc extracts with comparison to those treated with 50% extracts. As cell shrinkage and nuclei fragmentation were evident, the number of sites responsible for ROS formation, such as mitochondria, diminished considerably. Therefore, the ROS production may be, in fact, overshadowed by the occurring apoptosis/necrosis, as proven already by the examinations of adhesion, proliferation, and zinc-binding ability. We postulate that the less diluted extracts, i.e., >50% may result in cell death due to ROS overproduction. It is also worth noting that the DHE assay, like all fluorescent assays of these kinds, shows some cross reactivity and this might overestimate the signal.[46] On the other hand, bleaching of the probe might lead to an underestimation of the oxidative stress in cells.[47] In general, high reactivity of DHE probes do not make them exclusive to superoxide detection only.[48] $O_2^{\bullet-}$ gets bound easily to many molecules, generating RNS, including peroxynitrite, or secondary ROS, such as hydrogen peroxide, hydroxyl radicals as well as alkoxy radicals.[49] One of the most challenging hurdles to overcome in the context of DHE-based probes is the separation of 2-hydroxyethidium, the adduct of $O_2^{\bullet-}$ and DHE, from ethidium, an oxidation product of DHE.[48] Thus, it has to be borne in mind that the probe is specific for a wide spectrum of ROS, particularly $O_2^{\bullet-}$ and H_2O_2. Any change in the concentration of superoxide and its derivates should be viewed as indicative of alterations in oxidative chemistry within the investigated environment, rather than solely representing the precise formation of superoxide.
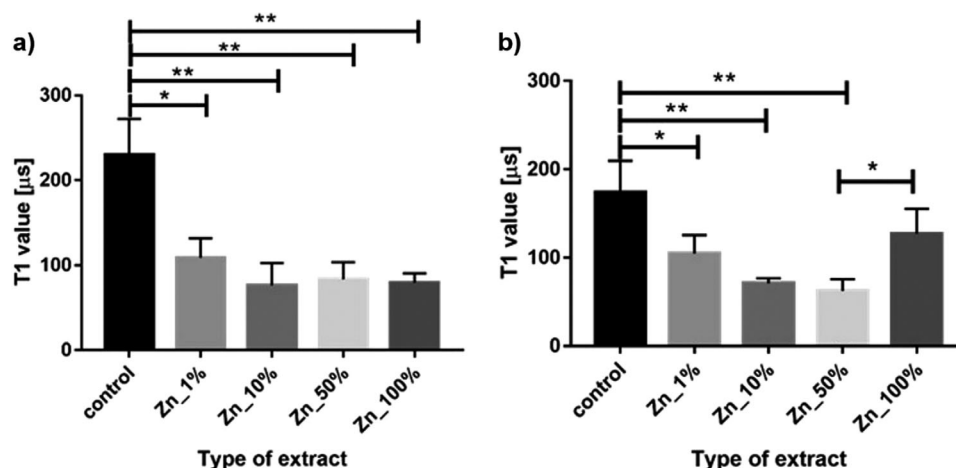
3.4. DAF-FM Assay

Figure 6 depicts the morphology of HUVECs treated with DAF-FM diacetate, a probe used to detect intracellular nitric oxide and its derivatives, whereas **Figure 7** illustrates the fluorescence intensity referenced to the control. Moreover, the estimated concentrations of RNS based on the approach described[32] are shown in

Figure S3 (Supporting Information). Analogously to the data obtained with the use of the DHE assay, we term the produced radical species as RNS, since, as discussed further, DAF-FM is not exclusive to detection of NO$^{\bullet}$. It may be observed that after exchanging the CCM with zinc-bearing extracts, the differences in fluorescence intensity between the control and the cells exposed to 1%, 10%, and 50% extracts were statistically insignificant, regardless of the incubation time. This indicates that the level of RNS produced in cells exposed to extracts of ≤ 50% metal concentration lies within the physiological level or that the assay is unable to detect RNS in HUVECs subjected to more diluted zinc-containing media. However, a surge in the generation of RNS was
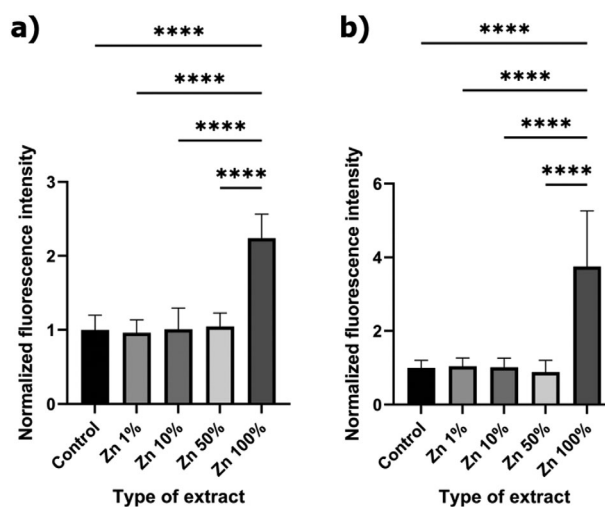
Figure 7. Normalized fluorescence intensity evaluated for cells treated with various zinc-containing extracts for a) 4 h, b) 24 h and the DAF-FM solution. Experiments were performed in six replicates for each variant. Data are presented as means ± standard ± standard deviation. The asterisks denote statistical significance (* $p < 0.05$, ** $p < 0.01$, *** $p < 0.001$, **** $p < 0.0001$).

**ADVANCED
SCIENCE NEWS**

www.advancedsciencenews.com

**ADVANCED
QUANTUM
TECHNOLOGIES**

www.advquantumtech.com

Figure 8. Relaxation time charts obtained after a) 4-h, b) 24-h incubation with zinc extracts. Experiments were performed in six replicates for each variant. Data are presented as means ± standard deviation. The asterisks denote statistical significance (* $p < 0.05$, ** $p < 0.01$, *** $p < 0.001$, **** $p < 0.0001$).

confirmed for 100% zinc extract, both after 4- and 24-h incubation. Moreover, in contrast to the generation of ROS, the longer the cells were cultivated in 100% zinc extracts, the more distinct production of RNS was noticed. Therefore, we believe the resulting cell death upon 4- or 24-h incubation with the CCM bearing the highest amount of zinc ions may be the result of the excessive generation of RNS. What also needs to be clarified is that even though the DAF-FM assays are being widely employed to measure intracellular nitric oxide, they in fact provide information about nitrosation of the studied environment.[48,50] The actual mechanism governing the reactions of DAF-FM with NO$^{\bullet}$ (or its oxidized adducts) to form benzotriazole inside cells remains a matter of debate. It may involve nitrosative (oxidation of NO$^{\bullet}$ to yield N_2O_3) and/or oxidative (one-electron oxidation of the reagent and subsequent reaction with nitric oxide) chemistry, which indicates that the probe might detect nitrosative reaction products of NO$^{\bullet}$, NO$^{\bullet}$ itself, or both.[48,51] Diaminofluoresceins are unable to separate the NO$^{\bullet}$-specific fluorescent signals given off by the triazole derivates from nonspecific fluorescent products created by reaction of a probe with, e.g., other biomolecules within cells or reagents that modifies the steady-state concentration of the intermediate radicals.[51] Thereby, dealing with DAF-FM assays should be viewed as monitoring the integrated intensity of nitrosative chemistry in a specific bioenvironment rather than the exact formation of NO$^{\bullet}$.[52]

3.5. Relaxometry

The T_1 values obtained for zinc-treated cells and zinc extracts are illustrated in **Figure 8** and Figure S4 (Supporting Information), respectively. The differences in relaxation times determined for zinc extracts were statistically insignificant indicating that zinc has no influence on the T_1 values measured in cells. As shown in Figure 8a, the T_1 values upon 4-h incubation were markedly lower for all the examined zinc-enriched cell cultures, in comparison to the reference group. It indicates that a larger amount of free radicals were formed upon exchanging the regular cell culture medium with the zinc-containing one. Strikingly, even

as low as 1% zinc extract caused the formation of radicals in endothelial cells. What is more, the differences between each of the tested conditions and the control group were statistically significant, indicating that abnormal amounts of zinc ions in CCM trigger the formation of intracellular free radicals. On the other hand, we did not observe any statistical significance in T_1 values between cells cultured in extracts of different concentrations. Such a tendency may be substantiated by the fact that relaxometry measurements provide nano-scale information from NV centers and their surroundings in diamonds distributed in various cellular compartments, not the data obtained by, e.g., mapping the entire cell. When the incubation time was prolonged to 24 h, a similar phenomenon was observed with the only exception being extracts containing 50% and 100% of zinc ions. The fact that the T_1 value detected for the 100% extract was not even statistically significant with respect to the control suggests that the level of radical species diminished considerably. As already shown in cell-material interaction studies and the analysis of assays designed for ROS/RNS detection, the cells maintained in 100% extracts no longer function properly as the phenomena related to cell death are apparent. Cell death-related processes observed upon treating HUVECs with 100% extracts might be a consequence of free radical generation.

4. Discussion

To the best of our knowledge, no reports linking the characterization of bulk biodegradable zinc and the generation of radical species were published. While optimizing the mechanical and corrosion properties of biomaterials, an in-depth assessment of their biological performance is required as well. Even though most of the in vivo studies do not document long-term, life-threatening toxicity of biodegradable zinc and its alloys,[1] some of the aspects, including possible overproduction of ROS/RNS, should be taken into consideration.

Henceforth, we refer to various literature studies concerned with 1) zinc and its anti-oxidative as well as pro-oxidative characteristics, 2) the impact of zinc excess on endothelial cells, and 3) relaxometry and its feasibility for radical species detection. Con-

**ADVANCED
SCIENCE NEWS**

www.advancedsciencenews.com

**ADVANCED
QUANTUM
TECHNOLOGIES**

www.advquantumtech.com

currently, based on the reported findings and phenomena as well as the results disclosed within the present study, we provide and discuss possible mechanisms mediating cell behavior subjected to high, non-physiological amount of zinc ions and the consequent formation of radical species, including superoxide, nitric oxide, and the common product of their reaction, peroxynitrite.

4.1. Zinc: An Antioxidant or a Prooxidant?

Under biological conditions, zinc remains in the Zn(II) valence state and, owing to its completely filled d shell, possesses redox-inert characteristics, hence it is unable to either oxidize or reduce any substance.[53] Zinc, at normal, physiological concentrations, contributes to the functioning of the antioxidant defense system by acting as an anti-inflammatory nutrient, which attenuates oxidative stress.[7]

Zinc serves as a co-factor for dozens of enzymes exhibiting antioxidative properties and hinders the activity of nicotinamide adenine dinucleotide phosphate oxidase (NADPH-Oxidase), a pro-oxidant enzyme. It also induces the synthesis of metallothioneins, proteins responsible for $OH^\bullet$ reduction and sequestration of ROS.[53,54] Even though zinc is an essential trace element, it turns into a toxin when is either released intracellularly from proteins or unbuffered, i.e., the concentration of zinc ions gets too high in a bio-environment. In both of these scenarios zinc homeostasis is perturbed and the element itself becomes a pro-oxidant.****[54] ROS formation from mitochondria, NADPH-Oxidase, or other sources may provoke intracellular zinc mobilization, resulting in a vicious circle of pro-oxidative conditions.[53] In fact, radical species-induced zinc liberation from cellular protein sites additionally exacerbates oxidative and nitrative injury, leading ultimately to cell death.[55] Within the present study, it may be assumed that elevated concentrations of zinc ions in endothelial cells, as shown by FluoZin-3 staining, do not entirely come from zinc-enriched media, but are also a consequence of zinc release from, e.g., metallothioneins as well.

The studies of zinc overload on neurons and astrocytes have shown that zinc-initiated cell death may be triggered by a host of phenomena, including the activation of NADPH-Oxidase and NOS, release of Zn^{2+} from proteins, inhibition of the mitochondrial respiratory chain and the resulting formation of free radicals, encompassing $O_2^{\bullet-}$, $NO^\bullet$, and $ONOO^-$.[53,56,57] As shown for hippocampal neurons, during oxidative stress, zinc concentration rises in lysosomes and brings about lysosomal dysfunction via membrane permeabilization and autophagy.[58] Consequently, released Zn^{2+} impedes the respiratory chain, hampers ATP synthesis, and increases the formation of ROS, which, in the end, affects the mitochondrial permeability transition pore (mPTP) and contributes to the release of apoptotic factors. Neuronal death occurs as a result of the excessive intracellular Zn^{2+}, mobilized and redistributed in a brain, not because of exogenous zinc.[53] One may suppose that similar outcomes could be achieved for endothelial cells overloaded with zinc ions.

Zinc homeostasis is regulated by two classes of zinc transport proteins, i.e., Zrt-/Irt-like proteins (ZIP) and zinc transporters (ZnT). The former is responsible for increasing the cytosolic zinc concentration, whereas the latter acts reversely as it manages the transport of zinc ions into various cellular compartments or the

extracellular space. The intracellular Zn^{2+} is distributed between the cytoplasm ($\approx 50\%$), nucleus ($\approx 30–40\%$) and the membrane (remainder). In addition, the majority of zinc ions are bound to proteins, such as proteins from the metallothionein family.[55,59] Mitochondria, lysosomes, and endoplasmic reticulum are the main organelles functioning as zinc stores, and they possess the ability to control the level of intracellular zinc. Nonetheless, when exposed to higher, non-physiological Zn^{2+} amounts, they may undergo mPTP opening and lysosomal membrane permeabilization (LMP). Both of these phenomena are well-established cell death mechanisms[9]. The mPTP opening causes depolarization, swelling, and cytochrome C release as well as caspase-dependent apoptosis, while the LMP provokes the release of cathepsins from the lysosomal lumen into the cytoplasm where the proteases participate in apoptosis signaling.[9,60] Within the present study, the detrimental effect of zinc ions on endothelial cells is especially striking upon loading them with 100% extracts, thus, the observed changes may be related to ZnT deficiency, protein dysfunction as well as mPTP and LMP.

The higher level of ROS in endothelial cells has been associated with endothelial dysfunction resulting eventually in cell death and the overall impaired neovascularization. Interestingly, it is Cu—Zn superoxide dismutase (SOD1), an antioxidant enzyme, which is mainly responsible for ROS scavenging in endothelial cells.[61,62] However, in pathological conditions, the cellular antioxidant may not be able to provide for a steady balance between free radical generation and neutralization. Deficiency of SOD1 leads to superior production of radical species, therefore, its activation ought to be viewed as an important defense mechanism against oxidative stress.[63] A hypothesis explaining the toxicity observed in this study is that the increased activity of SOD1 may be provoked in the cells exposed to 50% zinc extracts, considering that they generated the highest amount of ROS, including $O_2^{\bullet-}$, and yet still managed to grow and form agglomerates. We further hypothesize that the functioning of SOD1 was limited for the cells treated with 100% extracts. Therein, the largest level of RNS, such as $NO^\bullet$, was detected, though the formation of ROS diminished, either barely (4-h incubation) or considerably (24-h incubation). Since nitric oxide promotes dismutase activity in HUVECs,[64] we speculate that the protective properties of SOD1 might have weakened as a result of zinc excess and simultaneous overproduction of various free radicals provoking nuclei fragmentation, cell shrinkage, and bleb formation.

The explanation of cell death stemming from the use of 100% zinc extracts could be provided by the analysis of superoxide behavior. Mitochondria play a crucial role in respiration and they can also contribute to ROS generation since the respiratory chains contain a great deal of sites, i.e., complexes, where the one-electron reduction of oxygen takes place with a simultaneous formation of $O_2^{\bullet-}$. The matrix-generated superoxide can react with other molecules, e.g., $NO^\bullet$ or is converted to H_2O_2 by SOD. At high superoxide concentrations in cells, the reaction of hydrogen peroxide with iron-sulfur centers in proteins may provoke disadvantageous iron release. It is commonly known that as soon as iron ions are supplied, H_2O_2 may easily participate in Fenton reactions, leading to further generation of free radicals, such as highly toxic $HO^\bullet$. Ultimately, the functions of $O_2^{\bullet-}$ are not only restricted to additional, cascade-like induction of free radicals in redox signaling but also to nitric oxide inactivation as well as

**ADVANCED
SCIENCE NEWS**

www.advancedsciencenews.com

**ADVANCED
QUANTUM
TECHNOLOGIES**

www.advquantumtech.com

oxidative damage of different macromolecules, membranes, and DNA, via the production of more reactive, toxic ROS, including $ONOO^-$ and $HO^{\bullet}$.[59,65] With regard to ROS, it might be also postulated that Zn^{2+}, at high concentrations, could competitively displace iron and copper, two highly redox-reactive elements, from metal-binding domains, such as heme domains. Consequently, released cations might enable rapid catalytic conversion of molecular oxygen, generating ROS and inducing oxidative stress.[66] In this way, the production of free radicals should be viewed as zinc-initiated.

Up till now, the $NO^{\bullet}$ generation in endothelial cells was investigated mostly upon performing shear stress-based experiments.[32,67] In fact, it is well-known that endogenous $NO^{\bullet}$ production is mainly modulated by shear stress, being the product of blood velocity and shear rate.[68] Nitric oxide is naturally present in the environment of endothelial cells since it gets synthesized by endothelial nitric oxide synthase (eNOS), an enzyme of anti-apoptotic and cytoprotective abilities, thus acting as a crucial vascular protective gasotransmitter.[69] It has been reported that eNOS is especially prone to free calcium ions as it gets quickly phosphorylated and generates $NO^{\bullet}$ from L-arginine with L-citrulline as a reaction by-product.[68] One may hypothesize that a similar mechanism could be responsible for the larger production of $NO^{\bullet}$ in zinc-treated endothelial cells. In fact, a higher level of intracellular Zn^{2+} has been shown to correlate with the rise in intracellular Ca^{2+} concentration.[70] Within the present study, a dramatic increase in the generation of nitric oxide has been confirmed for HUVECs treated with 100% zinc extracts. These cells were not functioning properly anymore, thus the observed globular shape, fragmentation of nuclei, and cell shrinkage may be related to the overproduction of $NO^{\bullet}$ originating from free zinc excess. The disproportionate, high level of nitric oxide and its derivatives in cells is extremely cytotoxic. They may bring about mitochondrial protein tyrosine nitration, disturbing organelle homeostasis and, thereby, determining the cell fate.[71]

The production of $ONOO^-$ could also explain the morphology and behavior of cells exposed to 100% zinc extracts. $NO^{\bullet}$ naturally impedes superoxide production by the NADH/NADPH-Oxidase inactivation as well as endothelial SOD induction. However, as soon as the concentration of $O_2^{\bullet-}$ increases, $ONOO^-$ is generated and, as a consequence, lipid peroxidation and the nitrosation of amino acid residues occur.[72] Similar findings were reported while investigating zinc excitotoxicity. It has been shown that zinc tends to increase neuronal nitric oxides synthase expression as well as activity in neurons, resulting in an increase of $NO^{\bullet}$. Once nitric oxide gets bound to superoxide, the release of zinc from intracellular reservoirs occurs. Subsequently, ROS generation is induced with a wealth of side effects, encompassing mPTP opening, cytochrome C release, p38MAP kinase-mediated K+ efflux, and the final neuronal apoptosis9. What is also worth highlighting is that peroxynitrite is generated by eNOS under pathological conditions and is able to promote the formation of other free radicals, including $HO^{\bullet}$ or $^{\bullet}NO_2$, having a considerable impact on cell damage.[59,73] Zinc cations tend to attract peroxynitrite and, as a consequence, the zinc-thiolate cluster of eNOS gets oxidized with simultaneous release of zinc ions and the formation of disulfide bonds between the monomers.[73] It may be speculated that higher, non-physiological amount of Zn^{2+} in CCM leads to elevated concentrations of intracellular zinc

cations that, upon binding to $ONOO^-$, trigger a series of pro-oxidative and pro-nitrative reactions. Within the present study, a progressive rise in the intensity of Fluozin-3 fluorescence indicating the growing concentration of zinc in the intracellular space may substantiate the increased activity of Zn^{2+} and, probably, $ONOO^-$ harmful influence.

4.2. How do High Doses of Zinc Affect Endothelial Cells?

Reports covering zinc overexposure (regardless of how the element was administered) to endothelial cells and its pathological aftermath are scarce.[66,74,75] An increase in the level of intracellular zinc in pulmonary artery endothelial cells (PAECs) has been shown to mediate a series of events, including loss of mitochondrial integrity, elevation of mitochondrial-derived superoxide and induction of the apoptotic pathway. In the case of ROS and RNS formation in PAECs subjected to exogenously added zinc, they are believed to be brought about by high intracellular Zn^{2+} concentration combined with the inability of organelles to sequester excessive zinc ions from the cytosol.[66] Based on the data disclosed within the present study, it is possible to support such claims. The rise in the level of generated RNS corresponds with the increase in Zn^{2+} concentration, both in CCM and cellular environment, whereas the alterations of ROS amount upon exposure of HUVECs to zinc-enriched media might simply be affected by the processes of concurrent cell death.

Endothelial cells cultured in ions coming from biodegradable zinc samples were the subject of research by Ma et al.[74] The authors concluded that Zn^{2+} has a biphasic effect on the viability, proliferation, spreading as well as migration of human coronary artery endothelial cells (HCAECs). At low concentrations of zinc ions in CCM, these events are promoted, yet high amounts of Zn^{2+} lead to opposite outcomes. More recently, it has been reported that chronic exposure to relatively high doses of zinc results in accelerated senescence of HCAECs. Senescent HCAECs display altered homeostasis of zinc as manifested by its intracellular relocation and tend to undergo cell death upon short-term subjecting to large amount of Zn^{2+}.[75] Moreover, in senescent vascular smooth muscle cells, mitochondria are believed to be the sites of zinc accumulation, a phenomenon related to an increase in the generation of ROS.[76] Taking into account how high concentrations of zinc ions impacts PAECs and HCAECs, the alterations in the behavior of HUVECs, as observed within the present study, might be linked to ROS/RNS overproduction.

4.3. Relaxometry: A New Tool for the Analysis of Implant-Intended Materials

Overall, it has been suggested that superoxide and nitric oxide measurements within cells might need to be carried out in real time owing to the fact that these free radicals are extremely short-lived and reactive.[48] Live CLSM combined with subsequent image analysis provides insight into oxidative/nitrosative chemistry across cell organelles, yet the approach also suffers from a lot of drawbacks, e.g., biased microscopic view, changes in illumination, variability in contrast and brightness or light exposure-induced photobleaching of a dye.[77] This is where in the detection of free radicals one may benefit from the use of relaxometry

**ADVANCED
SCIENCE NEWS**

www.advancedsciencenews.com

**ADVANCED
QUANTUM
TECHNOLOGIES**

www.advquantumtech.com

(e.g., based on a stationary diamond), performed in a real-time mode. By using the technique, a limitless series of various experiments may be performed (as opposed to finite number of fluorogenic assays), localized intracellular measurements are possible and the overall method sensing performance stands out.[78]

Relaxometry could serve as an effective, powerful tool in monitoring the early cell response induced by any novel material. It has been previously shown that T_1 values are directly related to the concentration of free radicals, both in solution and in living cells.[22,32–35] In addition, it has been demonstrated that relaxometry can detect free radicals down to the nanomolar range.[79] By measuring known concentrations in solution, one can also estimate the concentration that would cause a certain shift in T_1.[79] Under pathological circumstances, such as the occurrence of non-physiological shear stresses,[32] viral infections,[34] or the presence of drugs,[35] free radicals generated in cells may be easily detected by this novel method and associated with the certain stimulus. The disproportionate amount of zinc ions in HUVECs exemplifies, as shown within the present study, an environment characterized by the constant production of ROS/RNS, clearly detrimental to cells. T_1 data provide complementary insight into material biocompatibility to the state of the art techniques. Further, we found that while the conventional assays showed a similar trend as the T_1 measurements, T_1 was more sensitive and could detect free radical generation at lower concentrations. Such higher sensitivity has already been shown before for other cell types.[80] However, it is not that directly comparable as it is sensitive to other chemicals, at a different time scale and length scale.

4.4. Summary and Future Perspectives

The presented study is the first-ever with respect to ROS/RNS production in endothelial cells originating from the use of biodegradable pure zinc. As shown, high zinc concentrations in HUVECs lead to their impaired growth, motility, significant radical species generation and, in worst-case scenario, cell death. The changes observed in endothelial cells subjected to 100% extracts may be a consequence of the excessive free radical production. The most plausible explanation is that high levels of intracellular zinc ions trigger the formation of ROS/RNS accompanied by a release of Zn^{2+} from various protein sites, eventually leading to free/labile zinc overload and cell death. The functioning of specific proteins is undoubtedly altered as a result of free radical generation stemming from zinc excess, yet as the phenomenon is not completely understood, it constitutes a part of another, ongoing study. While analyzing how intracellular Zn^{2+} overload stimulates ROS/RNS formation and subsequent oxidative/nitrosative stress, one needs to consider that it may be difficult to distinguish between zinc prooxidative activity and the innate oxidative stresses induced by other factors. As a matter of fact, the presence of excessive oxidants in any given system may exaggerate the role of increased zinc concentration.[53] Nevertheless, our study warrants further research on biocompatibility of zinc-based materials, especially from the point of view of radical species generation. In addition, whether cells actually undergo apoptosis/necrosis because of ROS/RNS production or free radicals are formed as a result of cell death needs to be examined as well. Therefore, while working on in vitro characterization of biodegradable zinc-

based materials it is advisable to either seek for or create novel protocols and implement different techniques, e.g., relaxometry as it provides complementary information to conventional assays or approaches. At the same time, it has to be borne in mind that performing experiments under static conditions do not necessarily represent those under dynamic conditions characteristic of living organisms. Overall, the data disclosed within the present study could serve as a benchmark for future studies in, e.g., biomaterials science or metallobiochemistry where the link between metals/ions and chemical/biological processes is unveiled.

5. Conclusions

Within the present study, endothelial cells were subjected to zinc-bearing extracts derived from pure biodegradable zinc, and four different concentrations of extracts were chosen in order to inspect the production of free radicals and the morphological changes in cells. The latter was studied first by using Confocal Laser Scanning Microscopy. Relaxometry based on NV centers in diamond was used to reveal the nano-scale impact of zinc ions on cells, i.e., the formation of intracellular free radicals. In addition, the DHE and DAF-FM assays combined with Live Confocal Laser Scanning Microscopy were implemented to detect reactive oxygen species (mainly superoxide) and reactive nitrogen species (nitric oxide and its derivatives) production, respectively. The obtained data enabled us to state that:

■ relaxometry is an effective, powerful tool in assessing cell responses to different pathological stimuli, including the excessive amount of metal ions. In combination with morphological studies, it provides complementary data about the impact of metal cations on cells.

■ the addition of 1% zinc extracts to cell cultures stimulates the production of free radicals as clearly confirmed by relaxometry studies.

■ the extracts containing up to 50% of zinc ions are generally well-tolerable by cells, although the normal cell shape, the formation of pseudopodia and cells agglomeration were mostly not noticeable for HUVECS exposed to 50% zinc extracts.

■ irrespective of the incubation time, the production of reactive nitrogen species was always most pronounced for cells subjected to 100% zinc extracts, whereas, in the case of reactive oxygen species, its largest concentration was detected for HUVECS exposed to 50% zinc extracts. The former may be one of the underlying reasons for the observed cell death, while the latter might evidence the inability of cells to grow properly and to form clusters.

■ the highest amount of zinc ions in culture medium leads to cell shrinkage, nuclei fragmentation, and bleb formation, being signs of inevitable cell death. The excessive zinc ions, coming from 100% extracts, are distributed in most of the remaining cell compartments. The observed phenomena may be a consequence of the overwhelming, zinc-induced production of reactive oxygen/nitrogen species.

Supporting Information

Supporting Information is available from the Wiley Online Library or from the author.

**ADVANCED
SCIENCE NEWS**

www.advancedsciencenews.com

**ADVANCED
QUANTUM
TECHNOLOGIES**

www.advquantumtech.com

Conflict of Interest

The authors declare no conflict of interest.

Author Contributions

D.W. and R.L. contributed equally to this work. All authors have given approval to the final version of the manuscript.

Data Availability Statement

The data that support the findings of this study are available from the corresponding author upon reasonable request.

[1] H. Kabir, K. Munir, C. Wen, Y. Li, *Bioact. Mater.* **2021**, *6*, 836.

[2] J. Jiang, J. Pi, J. Cai, *Bioinorg. Chem. Appl.* **2018**, *2018*, 1062562.

[3] S. V. Gudkov, D. E. Burmistrov, D. A. Serov, M. B. Rebezov, A. A. Semenova, L. A. B. A. Mini, *Front. Phys.* **2021**, *9*, 641481.

[4] A. L. Wani, N. Parveen, M. O. Ansari, M. F. Ahmad, S. Jameel, G. Shadab, *Curr. Med. Res. Pract.* **2017**, *7*, 90.

[5] N. Roohani, R. Hurrell, R. Kelishadi, R Schulin, *J. Res. Med. Sci.* **2013**, *18*, 144.

[6] B. Hennig, P. Meerarani, M. Toborek, C. J. McClain, *J Am Coll Nutr.* **1999**, *18*, 152.

[7] N. Marreiro D do, K. J. C. Cruz, J. B. S. Morais, J. B. Beserra, J. S. Severo, A. R Soares de Oliveira, *Antioxidants* **2017**, *6*, 24.

[8] T. Xia, M. Kovochich, M. Liong, L. Mädler, B. Gilbert, H. Shi, J. I. Yeh, J. I. Zink, A. E. Nel, *ACS Nano* **2008**, *2*, 2121.

[9] Y. H. Kim, J. W. Eom, J. Y Koh, *Front. Neurosci.* **2020**, *14*, 577958.

[10] A. L. Santos, S. Sinha, A. B. Lindner, *Oxid. Med. Cell. Longev.* **2018**, *2018*, 1941285.

[11] H. J. Shields, A. Traa, J. M. Van Raamsdonk, *Front. Cell Dev. Biol.* **2021**, *9*, 628157.

[12] L. A. Pavelescu, *J Med Life* **2015**, *8*, 38.

[13] K. S. Cujia, J. M. Boss, K. Herb, J. Zopes, C. L. Degen, *Nature* **2019**, *571*, 230.

[14] J. F. Barry, J. M. Schloss, E. Bauch, M. J. Turner, C. A. Hart, L. M. Pham, R. L. Walsworth, *Rev. Mod. Phys.* **2020**, *92*, 015004.

[15] R. Schirhagl, M. Loretz, C. L. Degen, *Annu. Rev. Phys. Chem.* **2014**, *65*, 83.

[16] I. Lovchinsky, A. O. Sushkov, E. Urbach, N. P. De Leon, S. Choi, K. De Greve, R. Evans, R. Gertner, E. Bersin, C. Müller, L. Mcguinness, F. Jelezko, R. L. Walsworth, H. Park, M. D. Lukin, *Science* **2016**, *351*, 836.

[17] S. Steinert, F. Ziem, L. T. Hall, A. Zappe, M. Schweikert, N. Götz, A. Aird, G. Balasubramanian, L. Hollenberg, J. Wrachtrup, *Nat. Commun.* **2013**, *4*, 1607.

[18] D. Le Sage, K. Arai, D. R. Glenn, S. J. Devience, L. M. Pham, L. Rahn-Lee, M. D. Lukin, A. Yacoby, A. Komeili, R. L. Walsworth, *Nature* **2013**, *496*, 486.

[19] J. P. Tetienne, T. Hingant, L. Rondin, A. Cavaillès, L. Mayer, G. Dantelle, T. Gacoin, J. Wrachtrup, J.-F. Roch, V. Jacques, *Phys. Rev. B: Condens. Matter Mater. Phys.* **2013**, *87*, 235436.

[20] F. C. Ziem, N. S. Götz, A. Zappe, S. Steinert, J. Wrachtrup, *Nano Lett.* **2013**, *13*, 4093.

[21] R. G. Monge, T. Delord, A. Lozovoi, N. V. Proscia, C. A. Meriles, *Bull Am Phys Soc* **2022**, *67*, Q39.

[22] F. P. Martínez, A. C. Nusantara, M. Chipaux, S. K. Padamati, R. Schirhagl, *ACS Sens.* **2020**, *5*, 3862.

[23] B. A. McCullian, A. M. Thabt, B. A. Gray, A. L. Melendez, M. S. Wolf, V. L. Safonov, D. V. Pelekhov, V. P. Bhallamudi, M. R. Page, P. C. Hammel, Ferromagnetic dynamics detected via one- and two-magnon NV relaxometry **2019**, preprint arXiv:1911.00829.

[24] A. Finco, A. Haykal, R. Tanos, F. Fabre, S. Chouaieb, W. Akhtar, I. Robert-Philip, W. Legrand, F. Ajejas, K. Bouzehouane, N. Reyren, T. Devolder, J.-P. Adam, J.-V. Kim, V. Cros, V. Jacques, *Nat. Commun.* **2021**, *12*, 767.

[25] S. K. Padamati, T. A. Vedelaar, F. P. Martínez, A. C. Nusantara, R. Schirhagl, *Nanomaterials* **2022**, *12*, 2422.

[26] J. Barton, M. Gulka, J. Tarabek, Y. Mindarava, Z. Wang, J. Schimer, H. Raabova, J. Bednar, M. B. Plenio, F. Jelezko, M. Nesladek, P. Cigler, *ACS Nano* **2020**, *14*, 12938.

[27] T. Rendler, J. Neburkova, O. Zemek, J. Kotek, A. Zappe, Z. Chu, P. Cigler, J. Wrachtrup, *Nat. Commun.* **2017**, *8*, 14701.

[28] T. Fujisaku, R. Tanabe, S. Onoda, R. Kubota, T. F. Segawa, F. T. K. So, T. Ohshima, I. Hamachi, M. Shirakawa, R. Igarashi, *ACS Nano* **2019**, *13*, 11726.

[29] A. Morita, T. Hamoh, F. P. Perona Martinez, M. Chipaux, A. Sigaeva, C. Mignon, K. J. van der Laan, A. Hochstetter, R. Schirhagl, *Nanomaterials* **2020**, *10*, 516.

[30] C. Reyes-San-Martin, T. Hamoh, Y. Zhang, L. Berendse, C. Klijn, R. Li, A. E. Llumbet, A. Sigaeva, J. Kawałko, A. Mzyk, R. Schirhagl, *ACS Nano* **2022**, *16*, 10701.

[31] L. Nie, A. C. Nusantara, V. G. Damle, R. Sharmin, E. P. P. Evans, S. R. Hemelaar, K. J. VAN DER LAAN, R. LI, F. P. Perona Martinez, T. Vedelaar, M. Chipaux, R. Schirhagl, *Sci. Adv.* **2021**, *7*, eabf0573.

[32] R. Sharmin, T. Hamoh, A. Sigaeva, A. Mzyk, V. G. Damle, A. Morita, T. Vedelaar, R. Schirhagl, *ACS Sens.* **2021**, *6*, 4349.

[33] N. Norouzi, A. Citra, Y. Ong, T. Hamoh, L. Nie, A. Morita, Y. Zhang, A. Mzyk, R. Schirhagl, *Carbon* **2022**, *199*, 444.

[34] K. Wu, T. A. Vedelaar, V. G. Damle, A. Morita, J. Mougnaud, C. R. San Martin, Y. Zhang, D. P. I. van der Pol, H. Ende-Metselaar, I. Rodenhuis-Zybert, R. Schirhagl, *Redox Biol.* **2022**, *52*, 102279.

[35] Y. Tian, A. C. Nusantara, T. Hamoh, A. Mzyk, X. Tian, F. P. Martinez, R. Li, H. P. Permentier, R. Schirhagl, *ACS Appl. Mater. Interfaces* **2022**, *14*, 39265.

[36] Y. Chen, P. Huang, H. Chen, S. Wang, H. Wang, J. Guo, X. Zhang, S. Zhang, J. Yan, J. Xia, Z. Xu, *ACS Biomater. Sci. Eng.* **2018**, *4*, 4095.

[37] H. Yang, B. Jia, Z. Zhang, X. Qu, G. Li, W. Lin, D. Zhu, K. Dai, Y. Zheng, *Nat. Commun.* **2020**, *11*, 401.

[38] O. A. Shenderova, A. I. Shames, N. A. Nunn, M. D. Torelli, I. Vlasov, A. Zaitsev, *J. Vac. Sci. Technol. B* **2019**, *37*, 030802.

[39] N. Mohan, C. S. Chen, H. H. Hsieh, Y. C. Wu, H. C. Chang, *Nano Lett.* **2010**, *10*, 3692.

[40] S. R. Hemelaar, B. Saspaanithy, S. R. M. L'Hommelet, F. P. Perona Martinez, K. J. van der Laan, R. Schirhagl, *Sensors* **2018**, *18*, 355.

[41] M. Chipaux, K. J. van der Laan, S. R. Hemelaar, M. Hasani, T. Zheng, R. Schirhagl, *Small* **2018**, *14*, 1704263.

[42] A. El-Sharkawey, M Fitzpatrick, Calculate the Corrected Total Cell Fluorescence (CTCF) using imageJ **2016**.

[43] M. Pelliccione, B. A. Myers, L. M. A. Pascal, A. Das, A. C. Bleszynski Jayich, *Phys. Rev. Appl.* **2014**, *2*, 054014.

[44] T. W. Turney, M. B. Duriska, V. Jayaratne, A. Elbaz, S. J. O'Keefe, A. S. Hastings, T. J. Piva, P. F. A. Wright, B. N. Feltis, *Chem. Res. Toxicol.* **2012**, *25*, 2057.

[45] W. N. Everett, C. Chern, D. Sun, R. E. McMahon, X. Zhang, W. J. A. Chen, M. S. Hahn, H.-J. Sue, *Toxicol. Lett.* **2014**, *225*, 177.

[46] E. Owusu-Ansah, A. Yavari, U Banerjee, A protocol for in vivo detection of reactive oxygen species **2008**.

[47] S. Bekeschus, J. Kolata, C. Winterbourn, A. Kramer, R. Turner, K. D. Weltmann, B. Bröker, K. Masur, *Free Radic. Res.* **2014**, *48*, 542.

[48] P. L. Zamora, F. A. Villamena, *Measuring Oxidants and Oxidative Stress in Biological Systems* (Eds. L. Berliner, N. Parinandi) Springer, Cham, *34* **2020**.

[49] C. A. Juan, J. M. P. de la Lastra, F. J. Plou, E. Pérez-Lebeña, *Int. J. Mol. Sci.* **2021**, *22*, 4642.

[50] M. N. Möller, N. Rios, M. Trujillo, R. Radi, A. Denicola, B. Alvarez, *J. Biol. Chem.* **2019**, *294*, 14776.

[51] M. M. Cortese-Krott, A. Rodriguez-Mateos, G. G. C. Kuhnle, G. Brown, M. Feelisch, M. Kelm, *Free Radical Biol. Med.* **2012**, *53*, 2146.

[52] J. Li, A. LoBue, S. K. Heuser, F. Leo, M. M. Cortese-Krott, *Nitric Oxide* **2021**, *115*, 44.

[53] S. R. Lee, *Oxid. Med. Cell. Longevity* **2018**, *2018*, 9156285.

[54] W. Maret, *Free Radical Biol. Med.* **2019**, *134*, 311.

[55] C. J. Stork, Y. V. Li, *Brain Edema XVI*, Vol. *121*, Springer, Cham, New York **2016**, 347.

[56] K. M. Noh, J. Y. Koh, *J. Neurosci.* **2000**, *20*, RC111.

[57] Y. H. Kim, J. Y. Koh, *Exp. Neurol.* **2002**, *177*, 407.

[58] J. H. Jung, S. J. Lee, T. Y. Kim, J. H. Cho, J. Y. Koh, *J. Neurosci.* **2008**, *28*, 3114.

[59] C. Hübner, H. Haase, *Redox Biol.* **2021**, *41*, 101916.

[60] A. C. Johansson, H. Appelqvist, C. Nilsson, K. Kågedal, K. Roberg, K. Öllinger, *Apoptosis* **2010**, *15*, 527.

[61] J. Groleau, S. Dussault, P. Haddad, J. Turgeon, C. Ménard, J. S. Chan, A. Rivard, *Arterioscler., Thromb., Vasc. Biol.* **2010**, *30*, 2173.

[62] A. Magenta, S. Greco, C. Gaetano, F. Martelli, *Int. J. Mol. Sci.* **2013**, *14*, 17319.

[63] I. Yokoyama, M. Negita, D. G. Liu, T. Nagasaka, T. Kobayashi, A. Hayakawa, S. Hayashi, A. Nakao, *Transplant Int.* **2002**, *15*, 220.

[64] H. Peng, S. Zhang, Z. Zhang, X. Wang, X. Tian, L. Zhang, J. Du, Y. Huang, H. Jin, *FEBS Open Bio* **2022**, *12*, 538.

[65] J. M. Li, A. M. Shah, *Am. J. Physiol.* **2004**, *287*, R1014.

[66] D. A. Wiseman, S. M. Wells, J. Wilham, M. Hubbard, J. E. Welker, S. M. Black, *Am. J. Physiol.* **2006**, *291*, C555.

[67] O. Yalcin, P. Ulker, U. Yavuzer, H. J. Meiselman, O. K. Baskurti, *Am J Physiol – Hear Circ Physiol.* **2008**, *294*, H2098.

[68] M. J. Simmonds, J. A. Detterich, P. Connes, *Biorheology* **2014**, *51*, 121.

[69] D. G. Duda, D. Fukumura, R. K. Jain, *Trends Mol. Med.* **2004**, *10*, 143.

[70] M. Saliani, R. Jalal, E. K. Goharshadi, *Nanomed. J.* **2016**, *3*, 1.

[71] W. J. Zenebe, R. R. Nazarewicz, M. S. Parihar, P. Ghafourifar, *J. Mol. Cell. Cardiol.* **2007**, *43*, 411.

[72] A. B. Levine, D. Punihaole, T. B. Levine, *Cardiology* **2012**, *122*, 55.

[73] M.-H. Zou, C. Shi, R. A. Cohen, *J. Clin. Invest.* **2002**, *109*, 817.

[74] J. Ma, N. Zhao, D. Zhu, *ACS Biomater. Sci. Eng.* **2015**, *1*, 1174.

[75] M. Malavolta, L. Costarelli, R. Giacconi, A. Basso, F. Piacenza, E. Pierpaoli, *Exp. Gerontol.* **2017**, *99*, 35.

[76] G. Salazar, J. Huang, R. G. Feresin, Y. Zhao, K. K. Griendling, *Free Radical Biol. Med.* **2017**, *108*, 225.

[77] D. M. Paul, S. P. Vilas, J. M. Kumar, *Nitric Oxide* **2011**, *25*, 31.

[78] A. Mzyk, A. Sigaeva, R. Schirhagl, *Acc. Chem. Res.* **2022**, *55*, 3572.

[79] A. Sigaeva, H. Shirzad, F. P. Martínez, A. C. Nusantara, N. Mougios, M. Chipaux, R. Schirhagl, *Small* **2022**, *18*, 2105750.

[80] R. Sharmin, A. C. Nusantara, L. Nie, K. Wu, A. E. Llumbet, W. Woudstra, A. Mzyk, R. Schirhagl, *ACS Sens.* **2022**, *7*, 3326.